Journal of Alloys and Compounds 509 (2011) 7042–7046

Contents lists available at ScienceDirect

Journal of Alloys and Compounds

journal homepage: www.elsevier.com/locate/jallcom

Processing and characterization of Sr doped $BiFeO_3$ multiferroic materials by high energetic milling

A. Moure*, J. Tartaj, C. Moure

Instituto de Cerámica y Vidrio, CSIC, C/Kelsen 5, 28049 Madrid, Spain

ARTICLE INFO

Article history:
Received 17 March 2011
Accepted 20 March 2011
Available online 20 April 2011

Keywords:
Bismuth ferrite
Multiferroic
Mechanosynthesis

ABSTRACT

Multiferroic ceramics based on $BiFeO_3$ and Sr-doped $BiFeO_3$ have been processed by high energetic milling and later thermal treatments at reduced temperatures to synthesize the perovskite structure. Single phase materials are obtained at 800 °C, reducing the temperature needed to complete the reaction in solid state method. Ceramics with densities higher than 94% were obtained at 1000 °C, and up to 98% at 1050 °C. All the ceramics were obtained in a single thermal treatment, where synthesis, grain growth and densification take place. The addition of Sr stabilizes the $BiFeO_3$ perovskite structure, avoiding its decomposition. Ceramics with higher dielectric permittivity and conductivity than non-doped materials are obtained, due to the increase of the amount of oxygen vacancies. It is shown for the first time that the grain boundary conductivity is increased in $BiFeO_3$ by doping with Sr.

1. Introduction

The term multiferroic is applied to those materials that present two or all three of ferroelectricity, ferromagnetism and ferroelasticity phenomena in the same phase [1], in such way that charges can be controlled by applied magnetic fields and spins can be controlled by applied voltages [2]. A major issue that makes the study of such materials difficult is the scarce number of phases that simultaneously present these properties. Particularly for ABO_3 oxides, a "$d^{0''}$ rule has been proposed to generally explain this fact [3]. Ferroelectricity appears for structures where B is occupied by transition metals with empty d shells. On the contrary, partially filled d shells are required for magnetism to occur. These are mutually exclusive phenomena that make difficult the appearance of multiferroism in such oxides. Even more scarce are the phases where these properties appear simultaneously at room temperature.

One of these few materials is $BiFeO_3$, where the polarization is mostly caused by the lone pair (s^2 orbital) of Bi^{3+}, so that the polarization comes mostly from the A site while the magnetization comes from the B site (Fe^{3+}), with a Neel temperature corresponding to its antiferromagnetic order of 370 °C and a ferroelectric Curie temperature of 820–830 °C [4]. Theoretical values of spontaneous polarization have been calculated by First-principles *ab initio* simulations to be close to 90 μC/cm^2 [5], and were measured to be as high as 40 μC/cm^2 in polycrystalline ceramics [6]. Antiferromagnetic characteristics are given by a spatially modulated spin structure that does not allow net magnetization and inhibits the observation of a notable linear magnetoelectric effect coupling between polarization (P) and magnetization (M). With the aim of induce net magnetic signal in $BiFeO_3$, substitution of Bi in A position by alkaline-earth elements as Sr has been successfully tested, and weak ferromagnetism has been proved to appear [7,8]. Important magnetoelectric effects, as the increase of the spontaneous polarization at increasing applied magnetic fields, have been observed in Sr-doped $BiFeO_3$ ceramics [9].

In addition to the appearance of magnetic improvements, the doping with Sr helps to stabilize the perovskite phase [10], which is one of the major issues in the study of these materials. Conventional [7] and rapid two-stage solid-state reaction [11] methods have been commonly used to process these materials, as well as sol–gel [12] or EDTA–citrate complexing process [13]. The appearance of secondary phases is also common in the processing of $BiFeO_3$ materials. With the aim of increasing the homogeneity in the constituent mixing and to make easier the processing of single phase perovskites, mechanical activation has been tested in this work. High energetic milling has been previously employed to facilitate the processing of $BiFeO_3$ [14] or B-doped $BiFeO_3$ materials [15]. To the author's best knowledge, the method has not been applied to Sr-doped $BiFeO_3$, where the presence of an additional cation in an A-site could complicate the processing of this material. The presence of $SrCO_3$ as raw material complicates the processing of the material with respect to $BiFeO_3$ in both classical and milling methods, as it is necessary to decompose the carbonate to incorporate Sr in the structure. Thus, differences with the pure bismuth ferrite material are expected in the mechanically activated process used here.

* Corresponding author.
E-mail address: alberto.moure@icv.csic.es (A. Moure).

0925-8388/$ – see front matter © 2011 Elsevier B.V. All rights reserved.
doi:10.1016/j.jallcom.2011.03.132

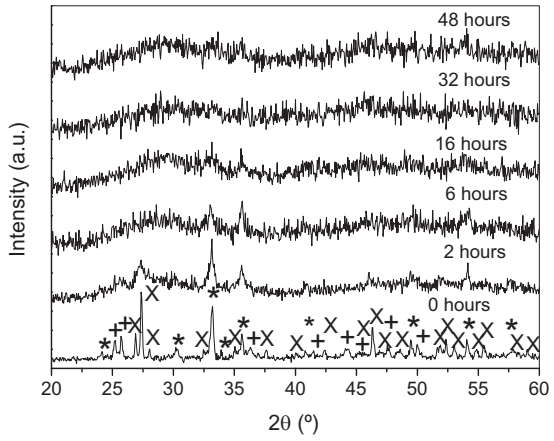

Fig. 1. XRD patterns of the stoichiometric mixture of Bi_2O_3, Fe_2O_3 and $SrCO_3$, precursor of $Bi_{0.60}Sr_{0.40}FeO_{2.8}$ ceramics after different milling times (X: Bi_2O_3; *: Fe_2O_3; +: $SrCO_3$).

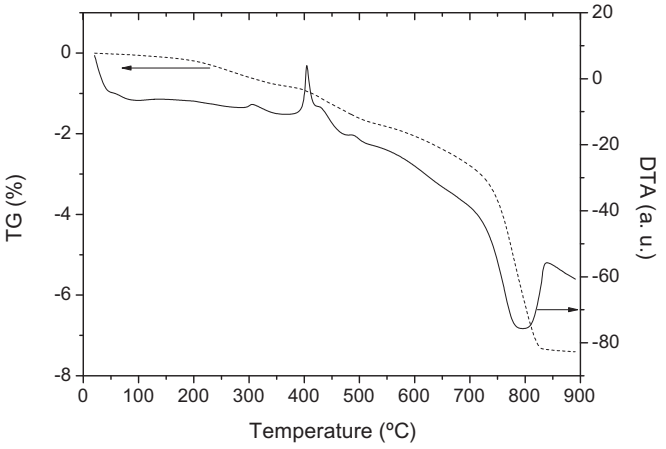

Fig. 2. DTA and TG curves of a mixture of Bi_2O_3, Fe_2O_3 and $SrCO_3$ after 48 h of milling.

In this work, ceramics with $Bi_{0.60}Sr_{0.40}FeO_{2.8}$ composition have been prepared by mechanical activation by means of high energetic milling and subsequent thermal treatments at low temperature. The high reactivity achieved during the mechanical treatment allows the sintering temperature to be lowered (<1100 °C). The ceramics were processed in a single thermal treatment, where synthesis, densification and grain growth take place, for the first time for this family of compounds. Dielectric permittivity and electrical conductivity were measured at room temperature, and the results explained as a function of the processing conditions.

2. Experimental

Stoichiometric quantities of Bi_2O_3, $SrCO_3$, and Fe_2O_3 necessary to obtain 4 g of the powdered ceramic phases with $Bi_{0.60}Sr_{0.40}FeO_{2.8}$ were placed in a stainless-steel pot with five also stainless-steel balls, 2 cm diameter (ball-to-powder weight ratio ~35/4). Mechanosynthesis was carried out with a Pulverisette 5 model Fritsch planetary mill operating at 250 rpm.

Evolution with different milling times of the precursors was monitored by Bragg-Brentano X-ray diffraction (XRD) with a Brüker AXS D8 Advance diffractometer. Cu K_α radiation ($\lambda = 1.5418$ Å) and a 5×10^{-2} deg $(2\theta)\,s^{-1}$ scan rate were used. Milled materials were treated at temperatures between 500 and 800 °C and characterized by XRD. The phases were identified using a scanning rate of typically 3.3×10^{-2} deg $(2\theta)\,s^{-1}$.

Approximately 0.7 g of the powders were uniaxially pressed in pellets with 0.8 mm diameter at 100 MPa and then isostatically pressed at 200 MPa. The shrinkage behavior was studied using a dilatometer Netzsch Gerätebau (model 402 EP, Selb-Bayern Germany) up to 1100 °C with a heating and cooling rate of 5 °C/min.

The pellets were then sintered in air at temperatures between 1000 and 1050 °C, and then characterized by XRD at the same conditions as for the precursors. The density of the ceramics was measured by Archimede's method in distilled water at room temperature. Impedance measurements were carried out by using a LF Impedance analyser (model HP-4294A, Hewlett-Packard) on disk pellets with electrodes of Ag (Dupont) calcined at 700 °C-1 h.

3. Results and discussion

Fig. 1 shows the diffraction patterns of the initial mixture and the powders milled at different times. The peaks corresponding to the oxides and the carbonate are broadened and with lower intensity after 2 h. They disappear after 32 h, where an amorphous material according to XRD analysis is obtained. This situation is maintained after 48 h of milling. That is, under these milling conditions, the mechanosynthesis of $Bi_{0.60}Sr_{0.40}FeO_{2.8}$ crystalline materials is not achieved. An increment in the milling time could lead to the mechanosynthesis of the material, but only after long mechanical treatments, and it is even possible that it is not achieved at these experimental conditions. In any case, 48 h of milling is long enough time to obtain this amorphous precursor powder. As it is known, the process of high energetic milling has been proved to increase the reactivity of the ceramic precursors even if mechanosynthesis does not occur [16]. Thus, powders after 48 h of milling were chosen for the further processing of the ceramics.

DTA and TG measurements were carried out on the materials milled during 48 h (Fig. 2). The total weight loss is 7.3% up to 830 °C, and it is maintained up to 900 °C. The major part of this loss comes from the decomposition of $SrCO_3$, which seems to remain after the prolonged milling. It has a theoretical value of 6.3%. The rest are due to the losses of CO_2 and H_2O adsorbed in the powder during the milling, which is a common feature in mechanically activated materials [17]. Bi losses up to 900 °C were not observed. An exothermic peak is observed at 400 °C, approximately, and a wide endothermic process also occurs between 760 and 830 °C, approximately. It is close to the melting point of Bi_2O_3, which is located at 825 °C [18], so can be related with it. The behavior observed in the DTA/TG curve is related with different processes occurring in the milled precursors.

Subsequent thermal treatments are necessary to synthesize the perovskite structure. Fig. 3 shows the diffraction patterns of the powders milled during 48 h after several thermal treatments at temperatures between 500 and 800 °C. At the lowest tested temperatures (500 °C), a mixture of initial precursors and a perovskite structured material is obtained. Thus, the exothermic peak in the DTA curve at 400 °C can be associated to the formation of the perovskite phase. The relatively high intensity of the $SrCO_3$ peaks indicates that most of the carbonate is not decomposed up to higher temperatures, in the order of 700 °C, as DTA curves indicate. The formed perovskite must have a composition close to $BiFeO_3$, as Sr

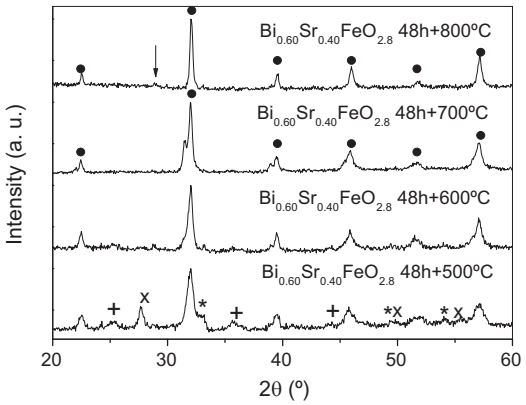

Fig. 3. XRD patterns after thermal treatments from 500 to 800 °C-1 h of the powder milled during 48 h. The points indicates the perovskite phase. The arrow indicates a trace of $Bi_2Fe_4O_9$.

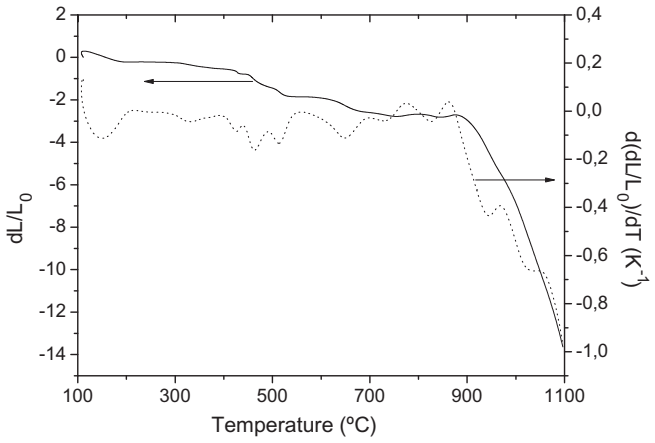

Fig. 4. Linear shrinkage and shrinkage rate of green pellets of $Bi_{0.60}Sr_{0.40}FeO_{2.8}$, from precursors obtained by mechanical activation after 48 h of milling.

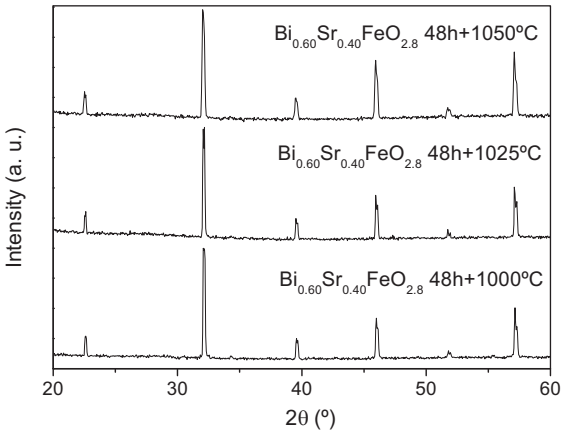

Fig. 5. XRD patterns of $Bi_{0.60}Sr_{0.40}FeO_{2.8}$ ceramics sintered from amorphous precursors obtained by after 48 h of milling.

is not incorporated until the $SrCO_3$ decomposes. In addition, a relatively high amount of Fe_2O_3 is present in the mixture. They react between them to produce a new phase (identified with a composition close to $SrFeO_{2.5}$, JCPDS 017-0932), observed at 600 °C and mostly at 700 °C, mixed with the $BiFeO_3$ perovskite. At 800 °C, the material is practically formed by the perovskite phase, without any other Sr compound, and only with traces of a secondary phase identified as $Bi_2Fe_4O_9$ (JCPDS 20-0836, marked with an arrow in Fig. 3), which is commonly observed in this system [8]. The formation of $Bi_2Fe_4O_9$ by Bi evaporation can be ruled out. Chen et al. [19] have detected this phase after heating at 160–180 °C, where Bi evaporation is not possible. Other authors state that this phase is a consequence of the decomposition of $BiFeO_3$. Recently, Selbach et al. [20] have described how this secondary phase is formed at 600–800 °C by decomposition of $BiFeO_3$, and disappears at higher temperatures, because Bi and Fe incorporate to the structure. They rule out any role of Bi evaporation, as traces would exist at increasing temperature, even in more amounts, which was not the case. Thus, a decrease of the synthesis temperature with respect to that needed by classical solid state reaction method (850–900 °C) [9,11] is obtained. The lowering of the synthesis temperature is in the order of that achieved by sol gel methods [21].

Fig. 4 shows the shrinkage curves (percentage and rate) of the ceramic precursors after milling during 48 h. Several shrinkage processes are observed up to approximately 875 °C. It was previously observed in other mechanosynthesized precursors, with $LaGaO_3$ composition and without using carbonates as initial raw materials [22]. They are related to the loss of H_2O and CO_2 trapped from the atmosphere in the mixture during milling. These phenomena can be also observed at the same temperatures range in the DTA/TG curves. The shrinkage is accelerated at a temperature close to 875 °C, and up to 1100 °C, where it has not yet finished. A similar behavior of other materials containing Bi, in which the shrinkage is not completed after the appearance of a liquid phase, has been previously reported [23]. The shrinkage rate presents at higher temperatures two maxima, the first located at 950 °C, and the second one at 1020 °C, approximately. It must be remarked that at those temperatures, according to the XRD patterns shown in Fig. 3, a major part of the mixture is formed by the perovskite phase. However, the shrinkage behavior seems to be associated with a liquid phase-assisting mechanism. The temperature at which the green pellet begins to shrink is close to the melting point of the Bi_2O_3. This means that at these conditions the non-reacted oxide is still present. It must be said that the measurement shown in Fig. 4 is dynamic, thus reactions taking time during 2 h, as the ones shown in Fig. 3, can be not completed. Despite this, small amounts of Bi_2O_3 can greatly modify the densification of the ceramics. It was recently reported that only a quantity of 0.5 wt% of Bi_2O_3 reduces in 200 °C the temperature of maximum shrinkage in $Ce_{0.9}G_{0.1}O_{1.95}$ ceramics, achieving densities higher than 99% [24]. The second maximum in the shrinkage rate curve located at 1020 °C fixes with the melting point of the $BiFeO_3$ perovskite [25]. It is not well defined, indicating that the amount of perovskite where Sr is not incorporated is low. It is known that the melting point of the bismuth ferrite increases with Sr content [7], and the maximum measured temperature shown in Fig. 4 is 1100 °C.

The results of the shrinkage measurements determine the conditions at which the ceramics are sintered. It was carried out at 1000, 1025 and 1050 °C. Higher temperatures were not tested, because the sintering at temperatures in the order of 1100 °C assisted by liquid phase can lead to inhomogeneous microstructures with abnormal grain growth [16]. The secondary phases observed after the thermal treatment and shown in Fig. 3 disappear when the ceramics are sintered at temperatures between 1000 and 1050 °C (Fig. 5). As it was mentioned above, the $BiFeO_3$ is really a not highly stable phase, which decomposes at approximately 600–800 °C in $Bi_2Fe_4O_9$ (as in Fig. 3) and $Bi_{25}FeO_{39}$ [20]. At higher temperatures, as those used during sintering in this work, the perovskite phase is formed again. The small amount of secondary phase observed indicates that the Sr helps to increase the stability of the perovskite phase [10].

Fig. 6 shows the total and apparent densities as a function of the sintering temperatures. An increase of the density is observed at increasing temperatures, with a maximum of a relative density close to 98% at 1050 °C. Measurements of the ceramics densities in $BiFeO_3$ compositions with Sr doping are barely found in the

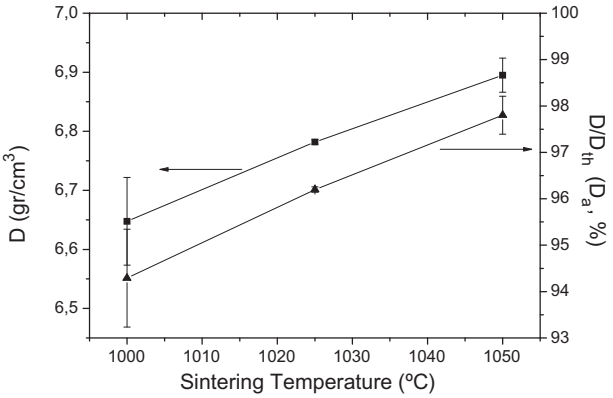

Fig. 6. Density and apparent density of $Bi_{0.60}Sr_{0.40}FeO_{2.8}$ ceramics measured by Archimedes's method.

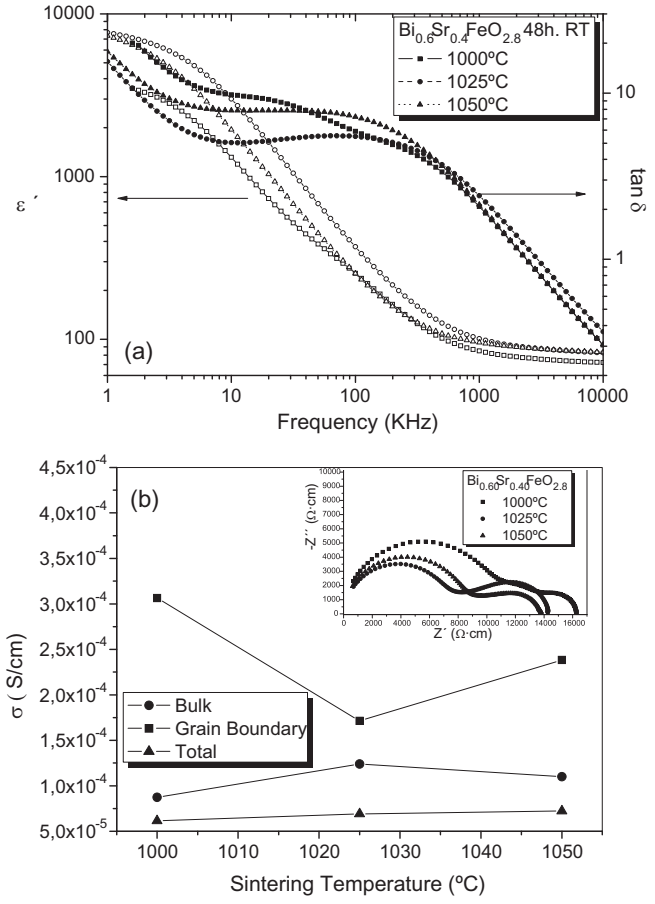

Fig. 7. (a) Real part of dielectric permittivity and dielectric loss factor at room temperature as a function of frequency of $Bi_{0.60}Sr_{0.40}FeO_{2.8}$ ceramics; (b) bulk, grain boundary and total dc conductivity at room temperature of $Bi_{0.60}Sr_{0.40}FeO_{2.8}$ ceramics (insets: Nyquist plots at room temperature from which conduction values were measured).

literature. Brinkman et al. reported in [10] maximum values of relative density of 96% for ceramics of $Bi_{0.5}Sr_{0.5}FeO_{3-\delta}$ composition sintered at 1100 °C. Classical solid state methods were used to obtain the ceramic precursors. The low melting point of Bi_2O_3 is a sintering aid that allows the processing temperature to be reduced, because it is a liquid-assisted process. It can be further diminished by the use of mechanical activation as in this work. The amorphization achieved after milling, caused by the decrease of the particle size and the introduction of large amounts of defects and strains, leads to a metastable and highly reactive state that promotes the mass transport and allows the sintering temperatures to be decreased. It must be remarked that this process is carried out in a single thermal treatment, where synthesis, sintering and grain growth take place. This is shown here for the first time in $BiFeO_3$-related compositions.

Fig. 7 shows the electrical characterization of the $Bi_{0.60}Sr_{0.40}FeO_{2.8}$ ceramics processed at different temperatures. Fig. 7a shows the dielectric permittivity and losses as a function of frequency at room temperature. Fig. 7b shows the values of grain, grain boundary and total conductivity, measured also at room temperature. In the inset, the Nyquist plots, from which the conduction features were calculated assuming a RC-RC equivalent circuit, are shown. The lowest values of dielectric permittivity correspond to the ceramic sintered at 1000 °C, which is also the one that presents the highest values of dielectric losses at the lowest frequencies.

The observed dispersion, with an important increase of both permittivity and dielectric losses at low frequencies, is a common feature in these compounds. It is a consequence of the appearance of oxygen vacancies. It is known that they are present in non-doped $BiFeO_3$ materials in relatively large amount [26], due to the deviation from stoichiometry [27]. There is an increase in the amount of oxygen vacancies with Sr doping, to compensate the charge difference between Sr^{2+} and Bi^{3+}. The increase in the dielectric permittivity at low frequencies is related with the appearance of dipoles created by the association of oxygen vacancies with doping cations. These dipoles can only be oriented under fields at low frequencies, contributing to the permittivity, but they cannot follow the electric field at higher frequencies. The value of the permittivity at 10 MHz (the highest frequency measured in this work) is 83, which is in the order of that found for similar Sr-doped $BiFeO_3$ (with values reported in the order of $\varepsilon_r \sim 100$ [11]. The values of permittivity at high frequencies are similar for the three ceramics. At low frequencies, the trend does not follow the curve of densification shown in Fig. 6. This indicates that other factors (grain size, crystallinity, even domain walls) different than the density determine the values of permittivity at those frequencies.

The presence of oxygen vacancies affects the conductivity and, as a consequence, the dielectric losses. The conductivity at room temperature shown here is in the order of $6–7 \times 10^{-5}$ S/cm, higher than those reported in [28] for $Bi_{0.8}Sr_{0.2}FeO_{3-\delta}$ (in the order of 10^{-6}) due to the higher content of Sr that increases the number of oxygen vacancies. The influence of doping can be appreciated by comparing with the conductivity of non-doped $BiFeO_3$, which is in the order of 10^{-10} S/cm [4]. The Nyquist plots allow the different contributions (bulk, grain boundary) to the total conductivity to be separated. It can be observed in Fig. 7b that the grain boundary and the bulk conductivity are in the same order, being slightly higher for the former than for the latter. The grain boundary conductivity in pure $BiFeO_3$ can be three orders of magnitude lower than the bulk one [29]. In view of the results shown in Fig. 7, it can be concluded that the doping with Sr increases the grain boundary conductivity, probably due to the increase of the amount of oxygen vacancies close to the grain boundary, together with a higher diffusivity associated with those interfaces. The conductivity is an important factor to be controlled in these materials, as it determines other properties as the leakage current [30], which deep study is out of the scope of this work.

4. Conclusions

The high energetic milling of precursors of $Bi_{0.60}Sr_{0.40}FeO_{2.8}$ in stainless-steel media produces an amorphous and highly reactive ceramic precursor that allows the synthesis temperature of this material to be reduced in 50–100 °C with respect to that needed by classical solid state method. The stability of the perovskite phase is increased due to the presence of Sr in the structure.

Ceramics with high relative density (up to 98%) are obtained at relatively low sintering temperature (1000–1050 °C) due to the high reactivity of the precursors and the probable aid of a liquid phase. The dielectric permittivity increases with respect to the pure bismuth ferrite, due to the influence of the oxygen vacancies. The conductivity is also higher for Sr-doped ceramics, due mainly to the increase of the grain boundary conductivity, in a result reported for the first time for these materials.

Acknowledgments

This work was supported by Spain PROFIT CIT-120000-2007-50 and MICINN MAT2008-06785-C02-02-E. Dr. A. Moure is indebted to the CSIC (MICINN) of Spain for the “Junta de Ampliación de Estudios” contracts (Refs. JAEDOC087).

References

[1] N.A. Hill, A. Filippetti, J. Magn. Magn. Mater. 242–245 (2002) 976–979.
[2] S.W. Cheong, M. Mostovoy, Nat. Mater. 6 (2007) 13–20.
[3] N.A. Hill, J. Phys. Chem. B 104 (2000) 6694–6709.
[4] G. Catalan, J.F. Scott, Adv. Mater. 21 (2009) 2463–2485.
[5] P. Ravindran, R. Vidya, A. Kjekshus, H. Fjellvåg, Phys. Rev. B 74 (2006) 1–18, 224412.
[6] V.V. Shvartsman, W. Kleemann, R. Haumont, J. Kreisel, Appl. Phys. Lett. 90 (2007) 1–3, 172115.
[7] J. Li, Y. Duan, H. He, D. Song, J. Alloys Compd. 315 (2001) 259–264.
[8] L.Y. Wang, D.H. Wang, H.B. Huang, Z.D. Han, Q.Q. Cao, B.X. Gu, Y.W. Du, J. Alloys Compd. 469 (2009) 1–3.
[9] B. Kundys, A. Maignan, C. Martin, N. Nguyen, C. Simon, Appl. Phys. Lett. 92 (2008) 1–3, 112905.
[10] K. Brinkman, T. Iijima, H. Takamura, Solid State Ionics 181 (2010) 53–58.
[11] V.A. Khomchenko, D.A. Kiselev, M. Kopcewicz, M. Maglione, V.V. Shvartsman, P. Borisov, W. Kleemann, A.M.L. Lopes, Y.G. Pogorelov, J.P. Araujo, R.M. Rubinger, N.A. Sobolev, J.M. Vieira, A.L. Kholkin, J. Magn. Magn. Mater. 321 (2009) 1692–1698.
[12] B. Bhushan, A. Basumallick, N.Y. Vasanthacharya, S. Kumar, D. Das, Solid State Sci. 12 (2010) 1063–1069.
[13] Y. Niu, J. Sunarso, W. Zhou, F. Liang, L. Ge, Z. Zhu, Z. Shao, Int. J. Hydrogen Energy 36 (4) (2011) 3179–3186.
[14] D. Maurya, H. Thota, K. Singh Nalwa, A. Garg, J. Alloys Compd. 477 (2009) 780–784.
[15] I.A. Santos, H.L.C. Grande, V.F. Freitas, S.N. de Medeiros, A. Paesano Jr., L.F. Cótica, E. Radovanovic, J. Non-Cryst. Solids 352 (2006) 3721–3724.
[16] A. Moure, L. Pardo, C. Alemany, P. Millán, A. Castro, J. Eur. Ceram. Soc. 21 (2001) 1399–1402.
[17] T. Hungria, A.B. Hungria, A. Castro, J. Solid State Chem. 177 (2004) 1559–1566.
[18] N.M. Sammes, G.A. Tompsett, H. Näfe, F. Aldinger, J. Eur. Ceram. Soc. 19 (1999) 1801–1826.
[19] C. Chen, J. Cheng, S. Yu, L. Che, Z. Meng, J. Cryst. Growth 291 (2006) 135–139.
[20] S.M. Selbach, M.A. Einarsrud, T. Grande, Chem. Mater. 21 (2009) 169–173.
[21] J. Wei, D. Xue, Electrochem. Solid State Lett. 10 (11) (2007) G85–G88.
[22] A. Moure, A. Castro, J. Tartaj, C. Moure, Ceram. Int. 35 (2009) 2659–2665.
[23] Z.S. Macedo, A.C. Hernandes, Mater. Lett. 59 (2005) 3456–3461.
[24] V. Gil, J. Tartaj, C. Moure, P. Duran, J. Eur. Ceram. Soc. 27 (2007) 801–805.
[25] A. Kumar, N.M. Murari, R.S. Katiyar, J. Raman Spectrosc. 39 (2008) 1262–1267.
[26] C. Ederer, N.A. Spaldin, Phys. Rev. B 71 (2005) 1–9, 224103.
[27] V.R. Palkar, J. John, R. Pinto, Appl. Phys. Lett. 80 (9) (2002) 1628–1630.
[28] V.A. Khomchenko, D.A. Kiselev, J.M. Vieira, A.L. Kholkin, M.A. Sá, Y.G. Pogorelov, Appl. Phys. Lett. 90 (2007) 1–3, 242901.
[29] S.V. Kalinin, M.R. Suchomel, P.K. Davies, D.A. Bonnell, J. Am. Ceram. Soc. 85 (12) (2002) 3011–3017.
[30] A.K. Pradhan, K. Zhang, D. Hunter, J.B. Dadson, G.B. Loutts, P. Bhattacharya, R. Katiyar, J. Zhang, D.J. Sellmyer, U.N. Roy, Y. Cui, A. Burger, J. Appl. Phys. 97 (2005) 1–4, 093903.